

Possible application of the optical tunnel effect to membrane biophysics

G. C. Bonazzola¹, G. Ciocchetti², E. Conte¹, A. De Marco^{1*}, M. Maringelli¹, and A. Trabucco¹

¹ Istituto di Fisica Superiore dell'Università di Torino, Corso Massimo D'Azeglio 46, I-10125 Torino, Italy

² Istituto di Fisica Teorica dell'Università di Torino, Torino, Italy

Received 11 June 1984/Accepted 16 January 1985

Abstract. The exploitation of the optical tunnel effect allows the detection of very small spatial variations. The theory of optical tunneling is extended to an absorbing medium and an experimental apparatus capable of detecting displacements down to 0.19 nm, with fluctuations equivalent to 0.10 nm, is described. Some possible applications to the measurement of electrically induced volume changes of biological membranes are discussed.

Key words: Microenvironments, total reflection, optical tunneling, membranes, excitable tissues

Introduction

It has been reported by many authors that the action potential in excitable cells is associated with small volume changes (Tasaki 1982; Cohen 1973; Tasaki and Iwasa 1982 a, b; Hill et al. 1977; Iwasa et al. 1980; Sandlin et al. 1968).

Cell wall movements have been found to lie between 5 and 10 nm in unmyelinated nerve fibers and to be about 100 nm in the fresh water alga, *Nitella* (Sandlin et al. 1968). There is now abundant evidence that the electric response of excitable membranes to a voltage stimulus is based on the operation of biological microdevices, known as ionic channels, capable of creating aqueous pores through the membrane. Their opening is responsible for the ionic currents associated with the action potential and these structures float in the fluid lipid phase which makes up the matrix of the membrane. The conformational changes which produce the opening of these channels are probably accompanied by volume changes (Conti et al. 1982 a, b). Changes in membrane thickness due to electrostriction have also been observed in artificial lipid bilayer systems (Benz and Janko 1976).

A method for detecting very small spatial variations can be developed by making use of the optical tunnel effect. Allegrini et al. (1971) have demonstrated that variations smaller than 0.10 nm in the gap between two optical surfaces can be measured by means of this effect. In the present work, after a brief summary of the theory of optical tunneling, we shall present some gap variation measurements and discuss some possible applications to membranes biophysics.

Theory of optical tunnel effect

The general concepts that are the basis of the optical tunnel effect can be found in several text books of Optical Physics. When total reflection of light occurs at the interface between two media (Fig. 1a), the electromagnetic field of the incident wave penetrates a short distance into the medium of lower refractive index, generating an "evanescent wave". This can be detected approaching the interface with a third medium at a distance ℓ , of the order of, or smaller than, the wavelength of the light, λ (Fig. 1b). Under the latter condition, energy propagation through medium 2 is induced and can be detected by a suitable third medium e.g. a lens (tunnel effect). The double discontinuity of the refractive index acts on photons as

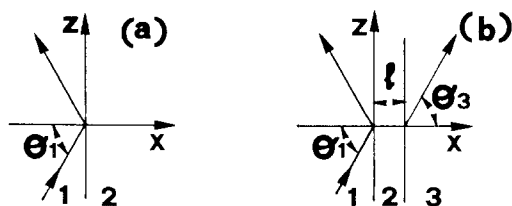


Fig. 1. a Total reflection on the surface separating media 1 and 2. b Optical tunnel effect caused by a third medium at distance ℓ from medium 1

* To whom offprint requests should be sent

a potential barrier for particles. A complete solution of Maxwell's equations is obtained by linking the solutions in the three media and taking into account the boundary conditions. This yields the following expressions for the transmission and reflection coefficients, T and R (see Appendix):

$$T = \frac{S}{1 + R_+ e^{2BX} + R_- e^{-2BX}} \quad R = 1 - T \quad (1)$$

where $X = 2\pi\ell/\lambda$.

The quantities S , R_+ , R_- , and B are functions of the refractive indexes (n_1 , n_2 , n_3), of the incidence angle, θ , and of light polarization, as shown in the Appendix.

Equation (1) has been derived by assuming that medium 3 is absorbing while media 1 and 2 are not. If medium 3 is non-absorbing, as is the case in the present work, $R_+ = R_-$. The position of maximum sensitivity depends mainly on the angle and the polarization of the incident light and on the absorption properties of medium 3. Therefore, for a given absorbing biological sample, an incidence angle and polarization state may be chosen in order to reach a suitable compromise between the required distance and the sensitivity.

Experimental apparatus

The above theory has been tested experimentally with the apparatus illustrated in Fig. 2.

The light beam was generated by a He-Ne Laser, ($\lambda = 632.8$ nm, Spectra Physics mod. 120) and impin-

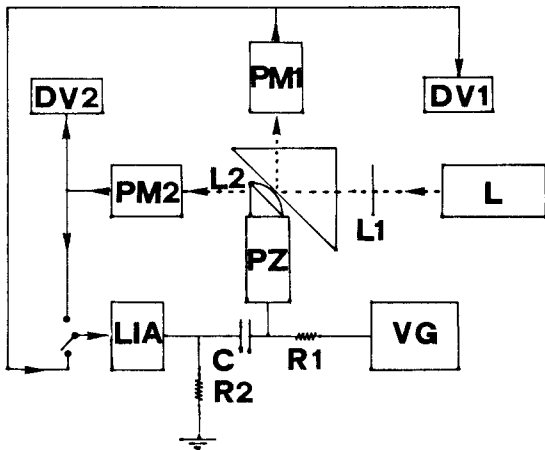


Fig. 2. Experimental set-up.

L = He-Ne laser; $DV1$, $DV2$ = Digital voltmeters; $PM1$, $PM2$ = Photomultipliers; LIA = Lock-in amplifier; VG = DC voltage generator; PZ = Piezoelectric translator; $L1$, $L2$ = Lenses; $R1 = 1M\Omega$, $R2 = 50K\Omega$, $C = 0.5 \mu F$

ged perpendicularly on the surface of a 45° prism (acting as medium 1, with $n_1 = 1.5085$), being focused by $L1$ on its diagonal face, where total reflection occurred. A small air gap (acting as medium 2, with $n_2 = 1$) separated this surface from the third medium, consisting of a small lens, $L2$, with $n_3 = 1.5051$. $L2$ was glued to a small supporting prism and fixed to a piezoelectric transducer (Physik Instrumente P172). $L1$ was used to reduce the beam diameter, but the convergence that it caused on the beam ($\pm 0.4^\circ$) had a negligible effect on the plane wave condition. Transmitted and reflected light were detected by two photomultipliers (Philips XP1017) at right angles. Care was taken to ensure linearity in the response of the photomultipliers. Mechanical disturbances were minimized by mounting the whole apparatus on an isolated table. The outputs of the photomultipliers were measured by digital voltmeters and fed alternatively to a Lock-in Amplifier (Par JB-5). The distance, ℓ , between media 1 and 3 was varied coarsely with a micromanipulator, while fine adjustments were obtained by varying the dc voltage applied to a piezoelectric transducer.

For the best resolution in gap variation measurements, the distance, ℓ , was finally modulated by the Lock-in Amplifier output reference signal. In this case the Lock-in Amplifier directly provided dT/dX or dR/dX . In the measurements presented here the Lock-in Amplifier reference frequency was 400 Hz and the averaging time constant on the output signal was 1 s.

Results

The measurements were performed by recording the photomultiplier output voltage, V_{yi} , and the dc voltage, V_{xi} , applied to the piezoelectric transducer, which is linearly related to the gap width.

These experimental values were normalized to the theoretical values of gap width and transmission or reflection coefficients by multiplying the V_{xi} 's by a scale factor a and shifting them by V_{xo} , and by multiplying the V_{yi} 's by a factor, K . The parameters a , V_{xo} and K were estimated experimentally and optimized by a Monte Carlo method. Theoretical curves (full-line) and experimental data (dots) for light transmission measurements are shown in Figs. 3 and 4, for two different polarization conditions of the incident light and a modulating signal amplitude corresponding to 1.9 nm.

In view of a possible application of this method to the study of biological samples, which are usually opaque, measurements of light reflection have also been carried out. Results of such a measurement are shown in Fig. 5, for a modulating signal amplitude corresponding to 1.9 nm. It is seen that the agreement of the data with the theoretical curves is

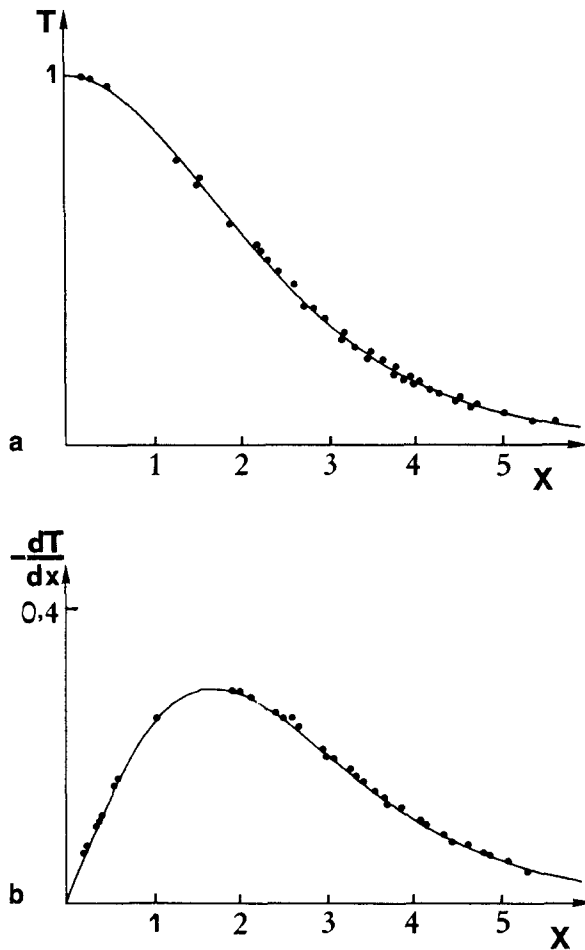


Fig 3. a Transmission coefficient versus distance between media 1 and 3, normalized to λ , with parallel light polarization. **b** Spatial derivate of the transmission coefficient versus distance between media 1 and 3, normalized to λ , with parallel light polarization

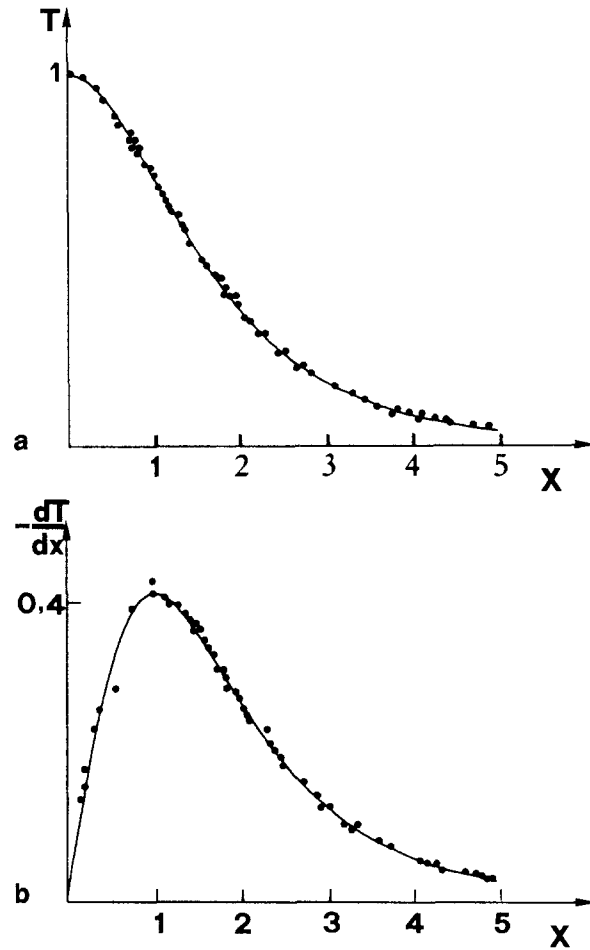


Fig. 4. a Transmission coefficient versus distance between media 1 and 3, normalized to λ , with perpendicular light polarization. **b** Spatial derivate of the transmission coefficient versus distance between media 1 and 3, normalized to λ , with perpendicular light polarization

slightly poorer than in the case of transmission measurements. Both transmission and reflection measurements were performed down to a modulating signal amplitude corresponding to 0.19 nm, at the same frequency of 400 Hz. In both cases the maximum fluctuation corresponded to 0.10 nm. Reducing the time of integration below 1 s caused higher fluctuations, thus affecting the value of the minimum displacement detectable by the derivative method with our apparatus. Fluctuations observed at the point of maximum sensitivity of the integral response, i.e. the photomultiplier output, were equivalent to 16 nm.

Discussion

The analytical method and experimental apparatus discussed above can be successfully used for measurements on biological samples, provided that the sample under examination is dipped in a suitable liquid.

The specimen must replace lens L2 in an experiment where only the reflected light is analyzed. Then medium 2 is the liquid and medium 3 is the biological sample. Moreover, a modified apparatus can be chosen if the specimen is expected to be damaged by mechanical vibrations and depending on the characteristics of the effect to be measured. The modulating signal could be used either

- a) to excite the sample electrically
- or
- b) to drive a piezoelectric transducer stuck to the prism, which is used as a vibrating probe; the other parts of the system remaining at rest.

Arrangement a) is convenient when volume changes are tunable to the frequency of the electric stimulus. They can be evaluated by detecting the reflected light and analyzing it with the Lock-in Amplifier locked at the same frequency and phase. With this adjustment our experimental apparatus could be used to detect volume changes in a nerve cell due to action

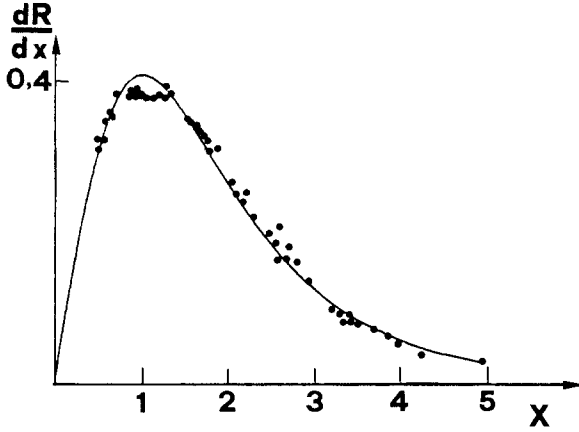


Fig 5. Spatial derivate of the reflection coefficient versus distance between media 1 and 3, normalized to λ , with perpendicular light polarization

potentials, as has already been observed using different techniques (Tasaki and Iwasa 1982a, b).

A second example of applicability of this technique is the measurement of electrically induced thickness changes (electrostriction) in artificial bilayers such as those measured by the capacitance method or by optical techniques (Benz and Janko 1976).

The detection of the changes of ionic channels in naked membranes of cultured cells is a more remote possibility, requiring a sensitivity to displacements of the order of 10^{-3} – 10^{-4} Å, a limit which has been achieved only with non-biological material, as reported by Allegrini et al. (1971).

Such a high sensitivity corresponds to the expected average change in membrane thickness, assuming a volume change of the order of 100 Å^3 per channel and about 100 channels per μm^2 (Conti et al. 1982a, b).

Obviously, arrangement a) cannot be applied to detect volume changes when an excitation frequency lower than 0.2 Hz is required, due to the low frequency limits of presently available Lock-in Amplifiers. In this case the technique of the vibrating prism should be chosen.

Arrangement b) could also be used if the biological sample responds with a random transient volume change, provided that its duration is sufficiently long compared with the minimum vibration period of the prism.

Acknowledgement. We wish to thank A. Borsellino and F. Conti for helpful discussions.

Appendix

Let us consider the propagation of plane electromagnetic waves through three plane and parallel layers with refractive indices n_1 , n_2 and n_3 . The quantities

n_1 and n_2 are real numbers (non-absorbing media) and $n_3 = n_{3R} (1 + i\chi)$ is in general complex (absorbing medium). Linking the solutions of Maxwell's equations in each homogeneous medium at the boundary surfaces, the following relation is obtained:

$$A_1^{(\pm)} = \frac{A_3^{(\pm)}}{2} (a_{\pm} \cosh(BX) \pm b_{\pm} \sinh(BX)), \quad (\text{A.1})$$

where $A_1^{(+)}$ and $A_1^{(-)}$ are the amplitudes of progressive and regressive waves in medium 1 and $A_3^{(+)}$ is the amplitude of the progressive wave in medium 3 and:

$$a_{\pm} = \frac{p_3}{p_1} \pm \frac{q_3}{q_1} \quad b_{\pm} = \frac{p_3 q_2}{p_2 q_1} \pm \frac{q_3 p_2}{q_2 p_1} \quad (\text{A.2})$$

$$B = q_2 q_2 / i = \sqrt{n_1^2 \sin^2 \vartheta_1 - n_2^2} \quad X = 2\pi \ell / \lambda \quad (\text{A.3})$$

ℓ = thickness of medium 2

λ = light wavelength in vacuum

The quantities p_i and q_i are defined in each medium, depending on the polarization mode of the incident light (electric field perpendicular (\perp) or parallel (\parallel) to the incidence plane), as follows:

$$\perp \text{ mode } \begin{cases} p_i = 1 \\ q_i = n_i \cos \vartheta_i \end{cases} \quad \parallel \text{ mode } \begin{cases} p_i = n_i \\ q_i = \cos \vartheta_i \end{cases}, \quad (\text{A.4})$$

where the angles ϑ_i are related by the Snell's law. The conditions for tunneling are:

$$\text{Re}(p_2 q_2) = 0 \quad \text{Re}(p_3 q_3) > 0. \quad (\text{A.5})$$

The first condition is equivalent to the well known condition for total reflection, $n_1 \sin \vartheta_1 > n_2$ and means that "evanescent waves" are standing in medium 2 because B in Eq. (A.1) is a real number. The second condition, Eq. (A.5), is a generalization of the condition $n_1 \sin \vartheta_1 < n_3$ for an absorbing third medium.

The relevant energy fluxes are in general given by:

$$\frac{c}{4\pi} |A_i|^2 \text{Re}(p_i q_i^*), \quad (\text{A.6})$$

where c is the light velocity in vacuum and transmission and reflection coefficients, denoted respectively by T and R , are calculated by dividing the progressive energy flux entering medium 3 and the regressive energy flux in medium 1 respectively, by the progressive energy flux in medium 1:

$$T = \left| \frac{A_3^{(+)}}{A_1^{(+)}} \right|^2 \frac{\text{Re}(p_3 q_3^*)}{\text{Re}(p_1 q_1^*)} \quad (\text{A.7})$$

$$R = \left| \frac{A_1^{(-)}}{A_1^{(+)}} \right|^2 \quad (\text{A.8})$$

By substituting the relations of Eq. (A.1) in the last expressions, one obtains:

$$T = \frac{S}{1 + R_+ e^{2BX} + R_- e^{-2BX}} \quad (\text{A.9})$$

$$R = T - 1 \quad (\text{A.10})$$

where:

$$R_{\pm} = \frac{1}{2} |a_{\pm} \pm b_{\pm}|^2 / (|a_{\pm}|^2 - |b_{\pm}|^2) \quad (\text{A.11})$$

$$S = 2(|a_{+}|^2 - |a_{-}|^2) / (|a_{+}|^2 - |b_{+}|^2). \quad (\text{A.12})$$

References

- Allegrini M, Ascoli C, Gozzini A (1971) Measurements of changes in length by an inhomogeneous wave device. *Opt Commun* 2:435–437
- Benz R, Janko K (1976) Voltage-induced capacitance relaxation of lipid bilayer membranes. Effect of membrane composition. *Biochim Biophys Acta* 455:721–740
- Cohen LB (1973) Changes in neuron structure during action potential propagation and synaptic transmission. *Physiol Rev* 53:373–410
- Conti F, Fioravanti R, Segal JR, Stuhmer W (1982a) The pressure dependence of the sodium currents of the squid giant axon. *J Membr Biol* 69:23–34
- Conti F, Fioravanti R, Segal JR, Stuhmer W (1982b) The pressure dependence of the potassium currents of the squid giant axon. *J Membr Biol* 69:35–40
- Hill BC, Schubert ED, Nokes MA, Michelson RP (1977) Laser interferometer measurement of changes in crayfish axon diameter concurrent with action potential. *Science* 195:426–428
- Iwasa K, Tasaki I, Gibbons R (1980) Swelling of nerve fibers associated with action potentials. *Science* 210:338–339
- Sandlin R, Lerman L, Barry W, Tasaki I (1968) Application of laser interferometry to physiological studies of excitable tissues. *Nature* 217:575–576
- Tasaki I (1982) *Physiology and electrochemistry of nerve fibres*. Academic Press, New York, pp 304–340
- Tasaki I, Iwasa K (1982a) Rapid pressure changes and surface displacements in the squid giant axon associated with production of action potentials. *Jpn J Physiol* 32:69–81
- Tasaki I, Iwasa K (1982b) Further studies of rapid mechanical changes in squid giant axon associated with action potential production. *Jpn J Physiol* 32:505–518